Kinetics of Inward-Rectifier K^+ Channel Block by Quaternary Alkylammonium Ions: Dimension and Properties of the Inner Pore

Donglin Guo and Zhe Lu

From the Department of Physiology, University of Pennsylvania, Philadelphia, Pennsylvania 19104

ABSTRACT We examined block of two inward-rectifier K^+ channels, IRK1 and ROMK1, by a series of intracellular symmetric quaternary alkylammonium ions (QAs) whose side chains contain one to five methylene groups. As shown previously, the ROMK1 channels bind larger QAs with higher affinity. In contrast, the IRK1 channels strongly select TEA over smaller or larger QAs. This remarkable difference in QA selectivity between the two channels results primarily from differing QA unbinding kinetics. The apparent rate constant for binding (k_{on}) of all examined QAs is significantly smaller than expected for a diffusion-limited process. Furthermore, a large (~30-fold) drop in k_{on} occurs when the number of methylene groups in QAs increases from three to four. These observations argue that between the intracellular solution and the QA-binding locus, there exists a constricted pathway, whose dimension (~9 Å) is comparable to that of a K^+ ion with a single H_2O shell.

KEY WORDS: ion selectivity • ion permeation • IRK1 • ROMK1 • TEA

INTRODUCTION

35 yr ago Armstrong and Binstock (1965) discovered that TEA intracellularly applied inhibits squid voltage-activated K^+ channels and thereby prolongs action potentials. This inhibition depends strongly on membrane voltage and, consequently, renders the channel inwardly rectifying, and is relieved by raising extracellular K^+ concentration or by membrane hyperpolarization (Armstrong and Binstock, 1965; Armstrong, 1971). Based on these observations, Armstrong (1971) proposed that intracellular TEA inhibits the channels by lodging in their inner pore. His proposal is supported by mutagenesis studies in the *Shaker* voltage-activated K^+ channels, which showed that mutations at some residues in the S6 segment lining the inner pore affect the binding of intracellular QAs, and that cysteine substituted at some S6 residues can be protected by TEA or tetrabutylammonium (TBA)[1] from chemical modification (Choi et al., 1993; Holmgren et al., 1997; del Camino et al., 2000). Armstrong (1971) also found that the TEA derivative nonyltriethylammonium (C9) can be trapped in the inner pore by the activation gate. Although the *Shaker* channel itself traps neither TEA nor decyltriethylammonium (C10) in the closed state, the I470C *Shaker* mutant channel is capable of trapping them both, as if the smaller cysteine side chain allows more room for TEA or C10 binding (Holmgren et al., 1997). Interestingly, *Shaker* residue I470 corresponds to a residue in the bacterial KcsA channel that lines the "cavity" internal to the narrow K^+-selective pore formed by the signature sequence (Doyle et al., 1998). Armstrong's (1971) model led him to propose that the inner pore diameter of voltage-activated K^+ channels is about that of TEA (~8 Å), comparable in size to a K^+ ion with a single H_2O shell. He further postulated that as they travel through the channels to the extracellular side, intracellular K^+ ions undergo two dehydration steps: (1) partial dehydration in the wider inner pore (~8 Å), and (2) full dehydration in the narrower and K^+-selective outer pore (~3 Å). However, the dimension of the inner pore in K^+ channels has since become an increasingly controversial subject.

French and Shoukimas (1981) found that the affinity of squid voltage-activated K^+ channels for larger symmetric quaternary alkylammonium ions (QAs), such as TBA (~10 Å) and tetrapentylammonium (TPeA; ~11 Å), is much higher than that for TEA. Similar phenomena were observed with ROMK1 inward-rectifier K^+ channels (Oliver et al., 1998; Spassova and Lu, 1998). Furthermore, using cysteine mutagenesis-based electrophysiological approaches, several laboratories have attempted to determine the dimension of the inner pore of inward-rectifiers, with intriguing results and potentially conflicting conclusions (Lu et al., 1999; Loussouarn et al., 2000). For example, based on their study in IRK1, Lu et al. (1999) suggest that the inner pore is so

Address correspondence to Dr. Zhe Lu, University of Pennsylvania, Department of Physiology, D302A, Richards Building, 3700 Hamilton Walk, Philadelphia, PA 19104. Fax: (215) 573-1940; E-mail: zhelu@mail.med.upenn.edu

[1]*Abbreviations used in this paper:* QA, quaternary alkylammonium ion; TBA, tetrabutylammonium; TMA, tetramethylammonium; TPeA, tetrapentylammonium, TPrA, tetrapropylammonium.

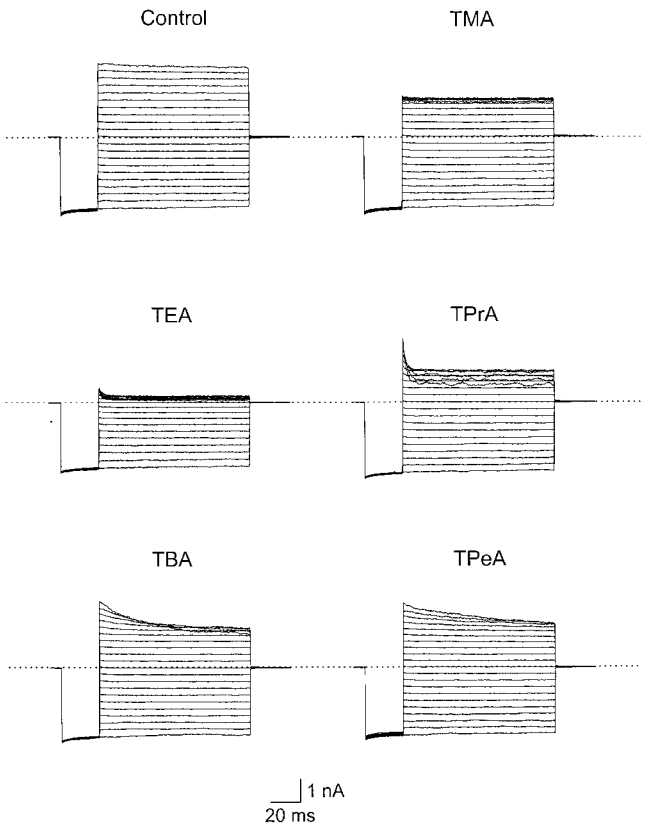

FIGURE 1. Block of IRK1 currents by intracellular QAs. Current traces without and with TMA, TEA, TPrA, TBA, or TPeA (each at 0.3 mM). The currents were elicited by stepping membrane voltage from the 0-mV holding potential to −100 mV (25 ms), and then to various test potentials (100 ms) from −100 to +100 mV in 10-mV increments. All current traces were recorded from the same patch and corrected for background current. The dotted lines identify the zero current levels.

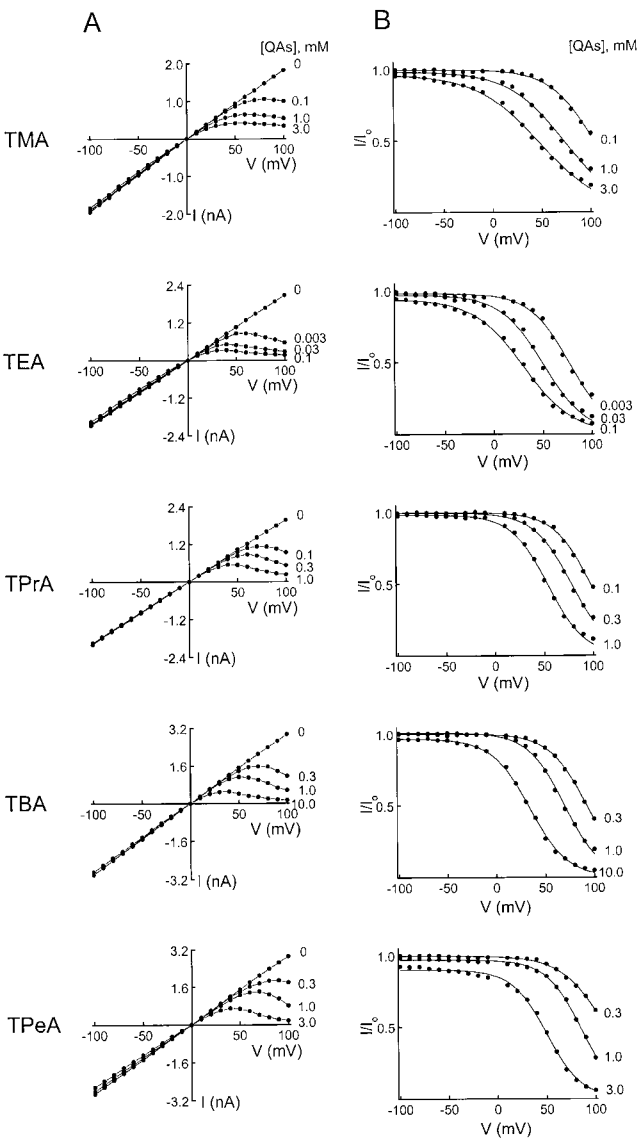

FIGURE 2. Effects of QAs on the I-V relationship of IRK1 channels. (A) Steady-state I-V curves without and with various concentrations of one of five QAs obtained from the data as shown in Fig. 1. The current was determined at the end of each test pulse. (B) Ratios of the I-V curves with and without the QAs shown in A. The curves superimposed on the data are fits of the equation $I/I_o = K_d/(K_d + [QA])$, where $K_d = K_d(0\ mV)e^{-ZFVm/RT}$. The $K_d(0\ mV)$ and Z values obtained from the fits are summarized in Fig. 9.

wide that it may not sustain single ion filing. These authors varied the number of cysteine substitutions and then examined how that number is related to the current reduction caused by intracellular methanethiosulfonate-ethyltrimethylammonium. They found that for some residues that presumably line the inner pore, several or sometimes all four equivalent residues needed to be replaced to obtain complete elimination of current by methanethiosulfonate-ethyltrimethylammonium. Based on this and other findings, they argue that the width of the inner pore can be >12 Å. On the other hand, Loussouarn et al. (2000) argue that the inner pore of the K_{ATP} channel (Kir6.2) can be as narrow as a few angstroms, because the four cysteine residues substituted at certain equivalent positions can be coordinated by a single Cd^{2+} ion. To gain some insight into the dimension of their inner pore, we systematically examined block of two inward-rectifier K^+ channels by a series of symmetric QAs.

MATERIALS AND METHODS

Molecular Biology and Oocyte Preparation

IRK1 and ROMK1 cDNAs were cloned into the pcDNA1/AMP and pSPORT plasmids, respectively (Ho et al., 1993; Kubo et al., 1993). IRK1 and ROMK1 RNAs were synthesized using T7 polymerase (Promega) from NotI-linearized cDNAs. Oocytes harvested from *Xenopus laevis* (*Xenopus* One) were incubated in a solution containing 82.5 mM NaCl, 2.5 mM KCl, 1.0 mM $MgCl_2$, 5.0 mM HEPES, pH 7.6, and 2–4 mg/ml collagenase. The oocyte preparation was agitated on a platform shaker (80 rpm) for 60–90 min, rinsed thoroughly, and stored in a solution containing 96

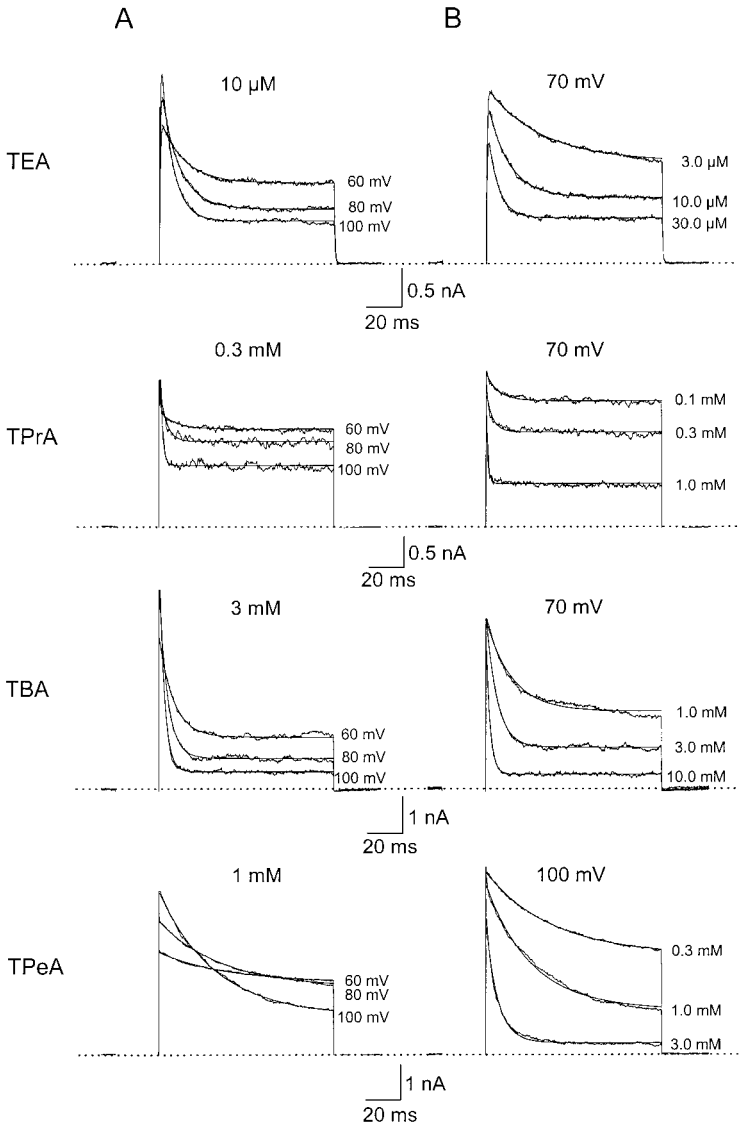

FIGURE 3. Kinetics of voltage jump–induced IRK1 current relaxations in the presence of QAs. (A) Current traces at three representative test voltages in the presence of a fixed concentration of a given QA. (B) Current traces at three representative concentrations of a given QA at a fixed test voltage. All current traces were collected as shown in Fig. 1, but for clarity, only the outward currents are shown.

mM NaCl, 2.5 mM KCl, 1.8 mM $CaCl_2$, 1.0 mM $MgCl_2$, 5 mM HEPES, pH 7.6, and gentamicin, 50 μg/ml. Defolliculated oocytes were selected and injected with RNA at least 2 and 16 h, respectively, after collagenase treatment. All oocytes were stored at 18°C.

Patch Recording

IRK1 and ROMK1 currents were recorded from inside-out membrane patches of *Xenopus* oocytes (injected with IRK1 cRNA) with a patch-clamp amplifier (model Axopatch 200B; Axon Instruments), filtered at 5 kHz, and sampled at 25 kHz using an analogue-to-digital converter (model DigiData 1200; Axon Instruments) interfaced with a personal computer. pClamp6 software (Axon Instruments) was used to control the amplifier and acquire the data. During current recording, the voltage across the membrane patch was first hyperpolarized from the 0-mV holding potential to −100 mV for 25–50 ms, and then stepped to a test voltage from −100 to +100 mV for a period of 0.1–1 s; the increment between consecutive test voltages was 10 mV. Background leak current correction was carried out as previously described (Lu and MacKinnon, 1994; Guo and Lu, 2000). During the recording, the tip of the patch pipet was immersed in a stream of intracellular solution exiting 1 of 10 glass capillaries (ID = 0.2 mm) mounted in parallel.

Recording Solutions

The pipet (extracellular) solution contained (in mM): 100 K^+ (Cl^- + HPO_4^{-2} + $H_2PO_4^-$), 0.3 $CaCl_2$, and 1.0 $MgCl_2$. The bath (intracellular) solution contained (in mM): 90 K^+ (Cl^- + HPO_4^{-2} + $H_2PO_4^-$), and 5 K_2EDTA. Both solutions were buffered at pH 7.6 with 10 mM phosphate (HPO_4^{-2} + $H_2PO_4^-$). The bath solutions containing QAs were prepared daily. All chemicals were purchased from Fluka.

RESULTS

Block of IRK1 Channels by Intracellular Quaternary Ammoniums

Fig. 1 shows macroscopic IRK1 current traces in the absence or presence of one of five symmetric QAs: tetramethylammonium (TMA), TEA, tetrapropylammonium (TPrA), TBA, or TPeA at membrane voltages from −100

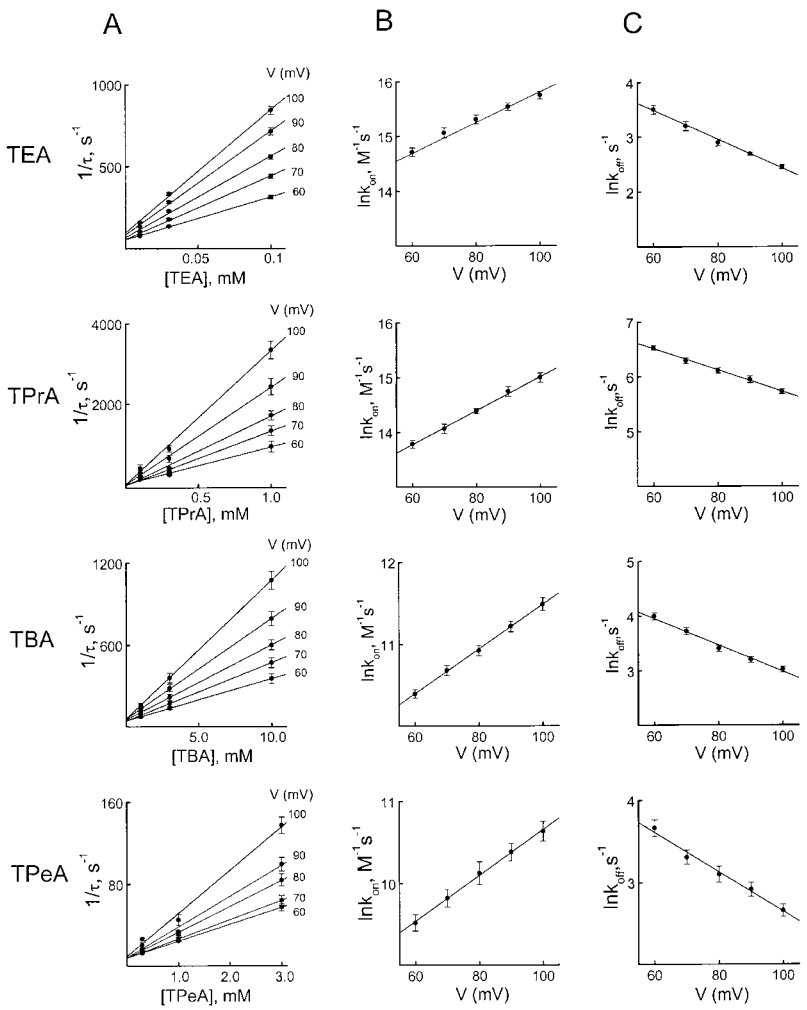

FIGURE 4. Analysis of the voltage jump–induced IRK1 current relaxations in the presence of QAs. (A) For a given QA, the reciprocals of the time constants ($1/\tau$; mean ± SEM, $n = 5$) obtained from the fits as shown in Fig. 3 are plotted against concentration and fitted with straight lines. (B and C) The natural logarithms of k_{on} and k_{off} (mean ± SEM, $n = 5$) are plotted against membrane voltage, respectively. The lines through the data are fits of the equation: $\ln k = \ln k(0\ mV) \pm zFV/RT$. The values of k(0 mV) and z thus obtained are summarized in Fig. 10.

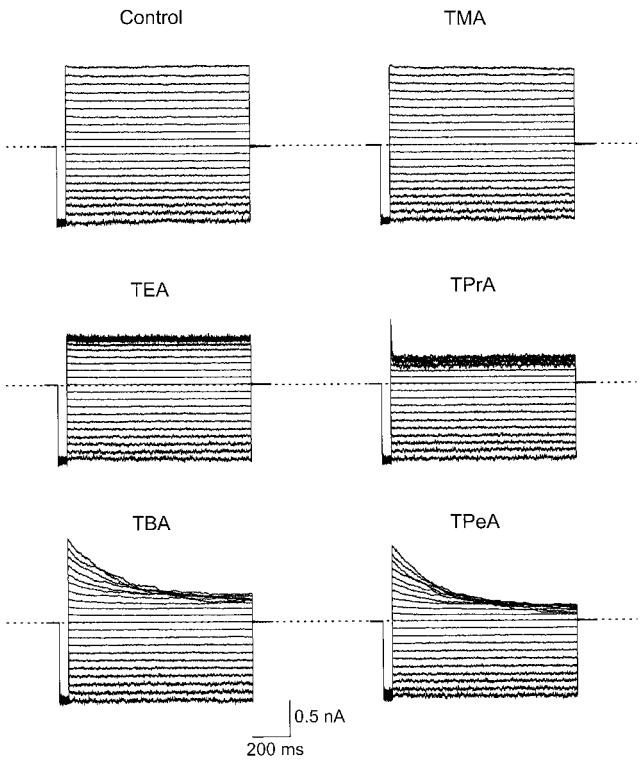

FIGURE 5. Block of ROMK1 currents by intracellular QAs. Current traces without and with TMA, TEA, TPrA, TBA, or TPeA (each at 0.3 mM). The currents were elicited by stepping membrane voltage from the 0-mV holding potential to −100 mV (50 ms), and then to various test potentials (1 s) from −100 to +100 mV in 10-mV increments. All records were obtained from the same patch.

to +100 mV in 10-mV increments. IRK1 exhibits a striking TEA selectivity: 0.3 mM TEA inhibited nearly all of the outward IRK1 current at positive voltages, whereas the other four QAs inhibited the IRK1 current much less strongly. Fig. 2 A shows I-V curves of IRK1 in the absence or presence of one of the five QAs at three representative concentrations. The extent of IRK1 block increased with QA concentration and membrane depolarization. The strongly voltage-dependent QA block rendered IRK1 inwardly rectifying. In Fig. 2 B, the fraction of unblocked IRK1 current in the presence of a given QA is plotted against membrane voltage at three representative QA concentrations. From fits of the Woodhull (1973) equation, we determined, for each QA, the K_d at 0 mV and the associated valence factor (Z).

Kinetics of Voltage Jump–induced IRK1 Current Transients in the Presence of Quaternary Ammoniums

Fig. 3 A shows the outward current transients induced by stepping membrane voltage from the −100-mV prepulse to the various test voltages indicated, in the presence of a fixed concentration of one of the four QAs (the kinetics of current transients in the presence of TMA are too fast to be resolved by our recording system; Fig. 1). Fig. 3 B shows current transients at several concentrations of one of the fours QAs but at a fixed test voltage. The smooth curves superimposed on the current records in both A and B are single-exponential fits. The reciprocal of the single-exponential time constant at a given test voltage is plotted against QA concentration in Fig. 4 A. Assuming that one QA molecule blocks one channel, we determined the apparent "on" rate constant (k_{on}) for the tested QA from the slope of the linear fit in Fig. 4 A and the "off" rate constant (k_{off}) from the product of k_{on} and the corresponding K_d. The natural logarithms of k_{on} and k_{off} are plotted against membrane voltage in Fig. 4 (B and C, respectively). The lines superimposed on the data in Fig. 4 (B and C) are fits of an equation, $\ln k = \ln k(0\text{ mV}) \pm zFV/RT$. From the fits, we determined k_{on} and k_{off} at 0 mV and the corresponding valence factors (z_{on} and z_{off}). Since the values of z_{on} and z_{off} for a given QA are comparable, the voltage dependence of the dissociation constant reflects a similar influence of membrane voltage on both k_{on} and k_{off}.

Block of ROMK1 Channels by Intracellular Quaternary Ammoniums

Fig. 5 shows the current traces of another inward-rectifier (ROMK1) in the absence or presence of one of five QAs, each at 0.3 mM, at membrane voltages from −100 to +100 mV in 10-mV increments. Contrary to our findings with IRK1, but consistent with previous reports, the extent of ROMK1 inhibition increases with increasing QA size (Oliver et al., 1998; Spassova and Lu, 1998). Fig. 6 A shows I-V curves of ROMK1 in the absence or presence of one of the five QAs at three concentrations. As in the case of IRK1, the extent of ROMK1 inhibition increased with both QA concentration and membrane depolarization. The strongly voltage-dependent QA block rendered ROMK1 inwardly rectifying. Fig. 6 B plots, for each QA, the fraction of unblocked ROMK1 current against membrane voltage at three concentrations. From the fits of the Woodhull equation we determined, for each QA, the K_d at 0 mV and the corresponding valence factor (Z).

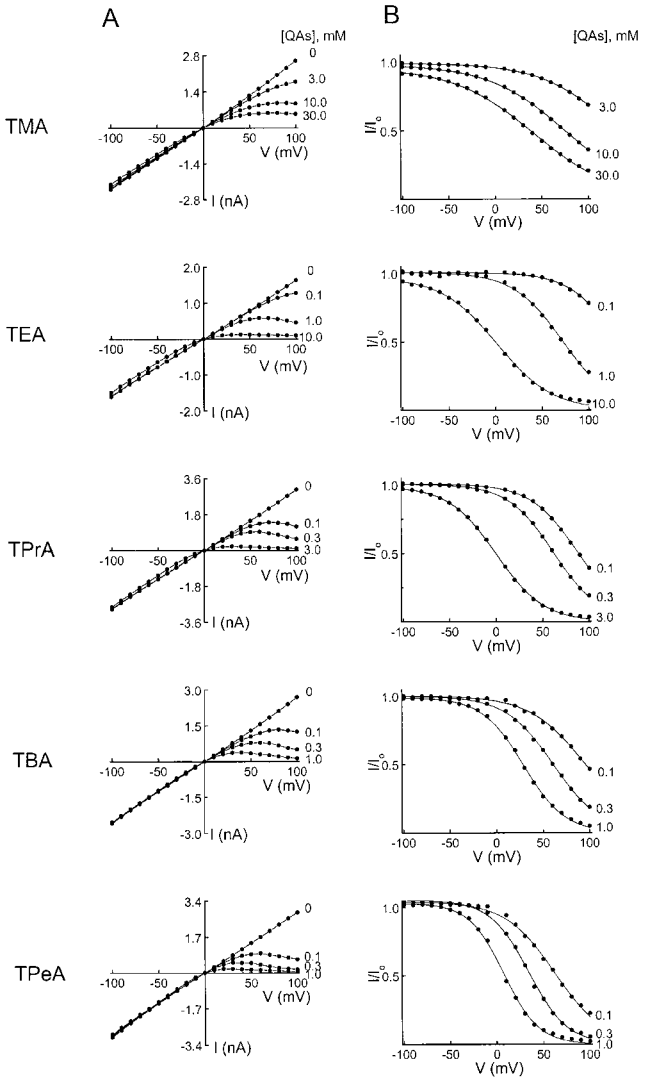

FIGURE 6. Effects of QAs on the I-V relationship of ROMK1 channels. (A) Steady-state I-V curves without and with various concentrations of one of five QAs, obtained from the data as shown in Fig. 5. (B) Ratios of the I-V curves with and without the QAs shown in A. The curves superimposed on the data are fits of the equation $I/I_o = K_d / (K_d + [QA])$, where $K_d = K_d(0\text{ mV})e^{-ZFV_m/RT}$. The $K_d(0\text{ mV})$ and Z values obtained from the fits are summarized in Fig. 9.

Kinetics of Voltage Jump–induced ROMK1 Current Transients in the Presence of Quaternary Ammoniums

Fig. 7 A shows current transients induced by stepping membrane voltage from the −100-mV prepulse to the

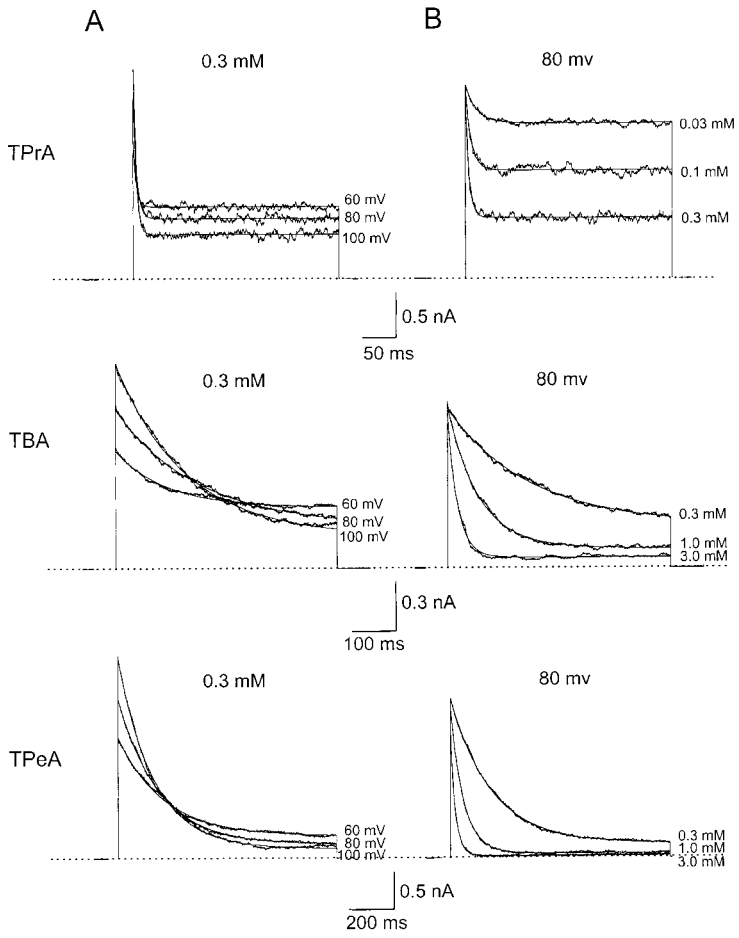

FIGURE 7. Kinetics of voltage jump–induced ROMK1 current relaxations in the presence of QAs. (A) Current traces at three representative test voltages in the presence of a fixed concentration of a given QA. (B) Current traces at three representative concentrations of a given QA at a fixed test voltage. All current traces collected as shown in Fig. 5, but for clarity, only the outward currents are shown.

various voltages indicated, in the presence of a fixed concentration of one of the three QAs (the kinetics of current transients in the presence of TMA or TEA is too fast to be resolved by our recording system; Fig. 5). Fig. 7 B shows the current transients recorded at various concentrations of a given QA but for a fixed test voltage. The smooth curves superimposed on the records in both A and B are single-exponential fits. The reciprocal of the single-exponential time constant at a given test voltage is plotted against the QA concentration in Fig. 8 A. Again, assuming that one QA molecule blocks one channel, we determined the apparent k_{on} for the tested QA from the slope of the linear fit in Fig. 8 A and k_{off} from the product of k_{on} and the corresponding K_d. The natural logarithms of k_{on} and k_{off} are plotted against membrane voltage in Fig. 8 (B and C, respectively); the lines superimposed on the data are fits of the equation used in Fig. 4. The fits yield k_{on} and k_{off} at 0 mV as well as corresponding z_{on} and z_{off}. It should be mentioned that when extrapolated to comparable conditions, k_{on} and k_{off} values for TPeA determined here are comparable to those reported by Oliver et al. (1998). As in the case of IRK1, the voltage dependence of the dissociation constant for QA binding to ROMK1 reflects the influence of membrane voltage on both k_{on} and k_{off}.

Comparison of Block of IRK1 and ROMK1 Channels by Quaternary Ammoniums

Fig. 9 A summarizes equilibrium dissociation constants K_d (0 mV) and the corresponding valence Z for the various QAs in both IRK1 and ROMK1. The affinity of ROMK1 for intracellular QAs increases with alkyl chain length, whereas IRK1 strongly selects TEA over smaller or larger QAs. Block of both IRK1 and ROMK1 by QAs is strongly voltage-dependent, although for each given QA the valence for IRK1 block is consistently larger (Fig. 9 B). Since the voltage dependence of block mostly reflects the movement, in the pore, of K^+ ions energetically coupled to the blocking ion, the Z value is greatly affected by the average number of K^+ ions in the pore (Spassova and Lu, 1998, 1999). The difference in Z value between the two channels may, therefore, largely reflect a difference in K^+ occupancy under our experimental conditions.

Fig. 10 summarizes rate constants k_{on} and k_{off} (0 mV) as well as corresponding valences z_{on} and z_{off} for several QAs in both IRK1 and ROMK1. For each QA, k_{on} is comparable in the two channels. Although k_{on} consistently

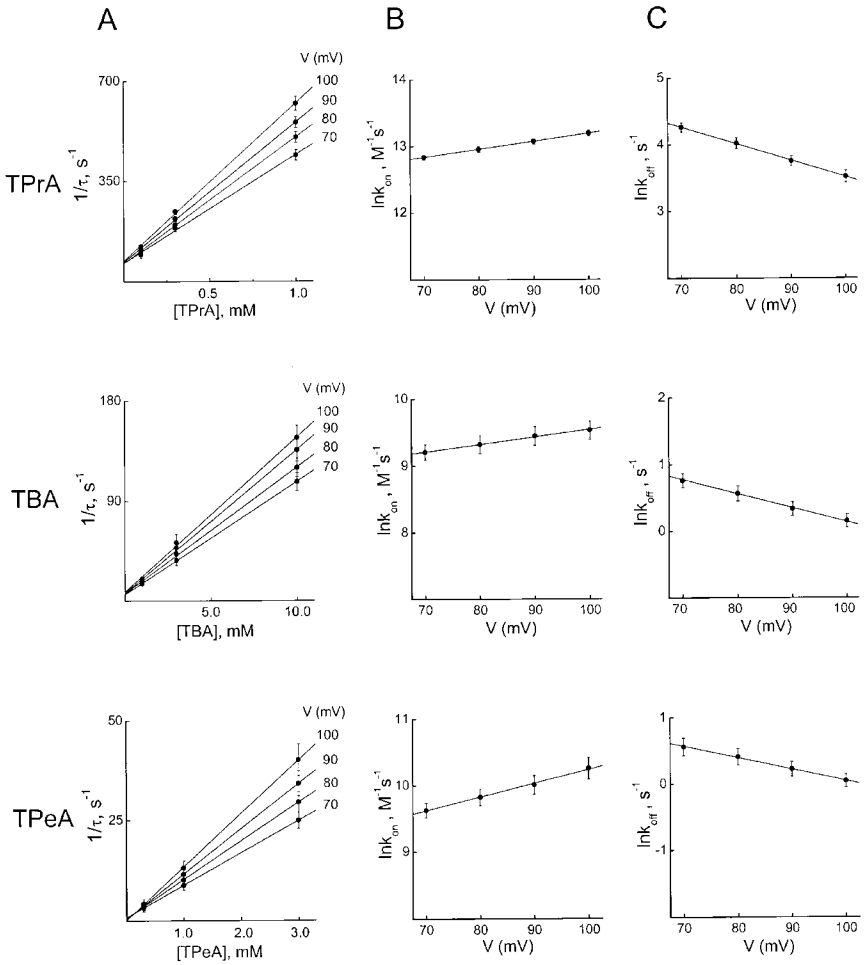

FIGURE 8. Analysis of the voltage jump–induced ROMK1 current relaxations in the presence of QAs. (A) For a given QA, the reciprocals of the time constants ($1/\tau$; mean ± SEM, $n = 5$) obtained from the fits as shown in Fig. 7 are plotted against the concentration and fitted with straight lines. (B and C) The natural logarithms of k_{on} and k_{off} (mean ± SEM, $n = 5$) are plotted against membrane voltage, respectively. The lines superimposed on the data are fits of the equation: $\ln k = \ln k(0\ mV) \pm zFV/RT$. The values of k(0 mV) and z thus obtained are summarized in Fig. 10.

decreases with increasing QA size (Fig. 10 A), the difference in k_{on} between TEA and TPrA or between TBA and TPeA is quite small (2–3-fold), whereas it is rather large (30-fold) between TPrA and TBA. Consequently, Fig. 10 A (note the logarithmic scale) shows an abrupt drop in k_{on} as QA size is increased above that of TPrA. As for k_{off}, in both channels, it decreases with increasing QA size (Fig. 10 C), except for TEA whose k_{off} (determinable in IRK1) is much smaller than expected from the general pattern. Values of k_{off} for TPrA, TBA, and TPeA are much larger in IRK1 than in ROMK1 (Fig. 10 B), accounting for the lower affinity of these three QAs for IRK1 (Fig. 9 A). Both k_{on} and k_{off} are voltage-dependent, with a little difference among QAs (Fig. 10, B and D). The values of z_{on} and z_{off} for IRK1 are comparable in magnitude, and similar to z_{off} for ROMK1, whereas z_{on} values for ROMK1 are lower (Fig. 10 B), which accounts for the stronger voltage dependence of channel block in IRK1 than in ROMK1 (Fig. 9 B).

Block of Mutant IRK1 and ROMK1 Channels by Intracellular Quaternary Ammoniums

The presence of an acidic residue in the second transmembrane (M2) segment of inward-rectifier K^+ channels is critical for the high affinity binding of intracellular Mg^{2+} and polyamines. Whereas aspartate is present at position 172 in IRK1, the corresponding residue (171) in ROMK1 is asparagine. The question arises whether the different QA selectivity in the two channel types simply reflects the presence of an acidic versus a neutral residue at that position. To test this possibility, we examined QA block of D172N-containing IRK1 and N171D-containing ROMK1 channels. Fig. 11 shows current records for the mutant channels in the absence or presence of 0.3 mM TMA, TEA, or TPrA (compare with Figs. 1 and 5). The resulting K_d (0 mV) and valences are plotted in Fig. 12 together with the corresponding ones for the wild-type channels already shown in Fig. 9. Neither mutation D172N in IRK1 nor mutation N171D in ROMK1 significantly affects channel block by any of the three QAs tested. Thus, the rather different QA selectivity between the two channels is not simply determined by the presence of the aspartate residue in the M2 segment.

DISCUSSION

The goal of the present study is to use QAs to probe the dimension of the inner pore of inward-rectifier K^+

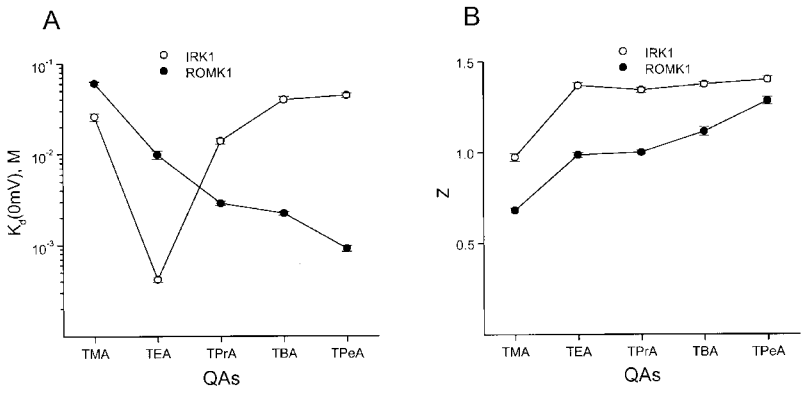

FIGURE 9. Summary of equilibrium dissociation constants and corresponding valence factors of channel block by QAs. The K_d(0 mV) and Z values (mean ± SEM, $n = 5$) for each QA, obtained as shown in Figs. 2 and 6, are presented in A and B, respectively. The open and closed circles correspond to the data for IRK1 and ROMK1, respectively.

channels. We incidentally observed an unexpected phenomenon: IRK1 exhibits a much higher affinity for intracellular TEA than for smaller or larger QAs, whereas ROMK1 binds larger intracellular QAs with higher affinity. The kinetic mechanism underlying the dramatic difference in QA selectivity between the two channels appears to be straightforward: it is conferred almost entirely by different QA unbinding kinetics (Fig. 10). On the other hand, the structural basis of the phenomenon remains unclear. It is not due to the presence of acidic aspartate (D172) in IRK1 versus neutral asparagine (N171) in ROMK1 (Figs. 11 and 12), even though an acidic residue at that position is critical for the high affinity binding of intracellular Mg^{2+} and polyamines (Ficker et al., 1994; Lopatin et al., 1994; Lu and MacKinnon, 1994; Stanfield et al., 1994; Fakler et al., 1995; Yang et al., 1995). Additional studies are needed to uncover the structural basis underlying the striking difference in QA selectivity between IRK1 and ROMK1. This difference suggests that inward-rectifiers, which play important physiological and pathophysiological roles, can be differentially targeted by low molecular weight pharmacological agents.

Returning now to the original question—the diameter of the inner pore—we use the term "inner pore" either literally or to refer to its narrowest part if the width is nonuniform. In practice, determining the inner pore diameter can be translated into identifying the largest ion that can readily enter it (Hille, 1971). In principle, if the inner pore were a stiff pipe and the test ions incompressible balls of various sizes (i.e., a system without compliance or friction) one would expect a simple binary outcome (Fig. 13 A): all ions smaller than the pore enter it with the same rate whereas larger ones are ex-

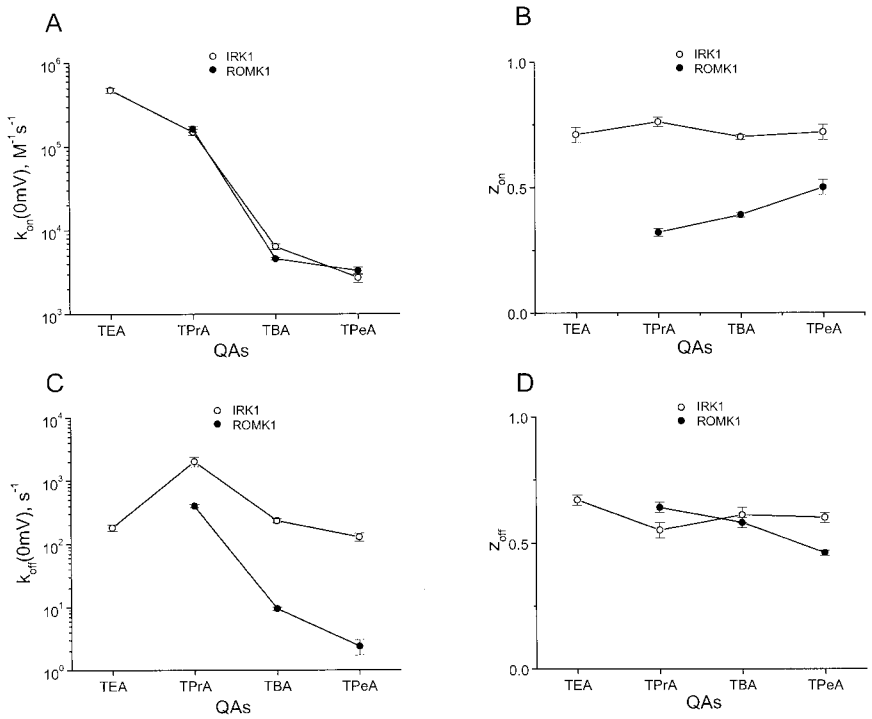

FIGURE 10. Summary of the rate constants and associated valence factors for channel block by QAs. The k_{on} and k_{off} values (mean ± SEM, $n = 5$) for a given QA are presented in A and C, and the z_{on} and z_{off} in B and D, respectively. The open and closed circles correspond to the data for IRK1 and ROMK1, respectively.

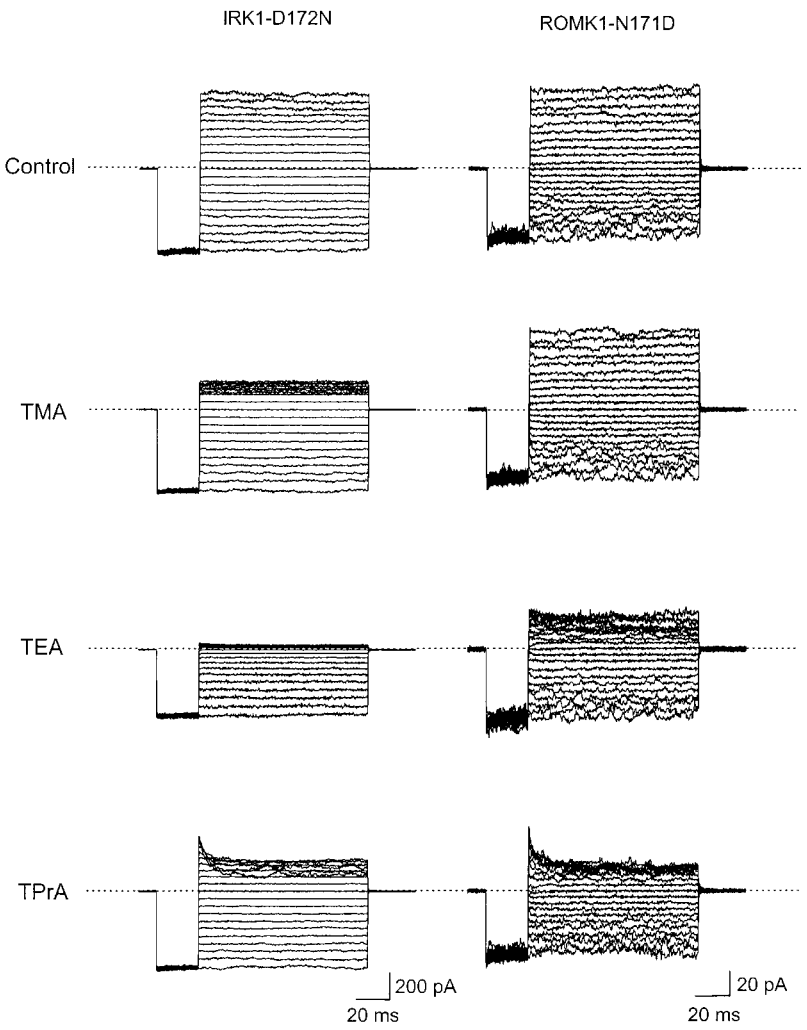

FIGURE 11. Block of mutant IRK1 and ROMK1 channels by intracellular quaternary ammoniums. IRK1-D172N and ROMK1-N171D current traces without and with TMA, TEA, or TPrA (each at 0.3 mM). The currents were elicited by stepping membrane voltage from the 0-mV holding potential to −100 mV (25 ms), and then to various test potentials (100 ms) from −100 to +100 mV in 10-mV increments. For each channel type, all records are from the same patch and corrected for background current.

cluded. Pore size would be identified as that of the largest ion that can enter, regardless of absolute entry rate.

However, the system (the inner pore and the QAs) that we studied exhibits compliance and hindrance. For example, uncertainty regarding absolute QA dimension increases with size; larger QAs may widen the pore as they elbow their way into it. Furthermore, as the QA travels towards its binding site, part of the longer alkyl chains may interact with and penetrate the netlike protein lining of the inner pore, significantly hindering the QA's mobility. Because of these effects, an ion larger than the normal size of the open pore may be able to squeeze into it but with a lower rate of entry (Fig. 13 B). Therefore, to determine the normal pore diameter one

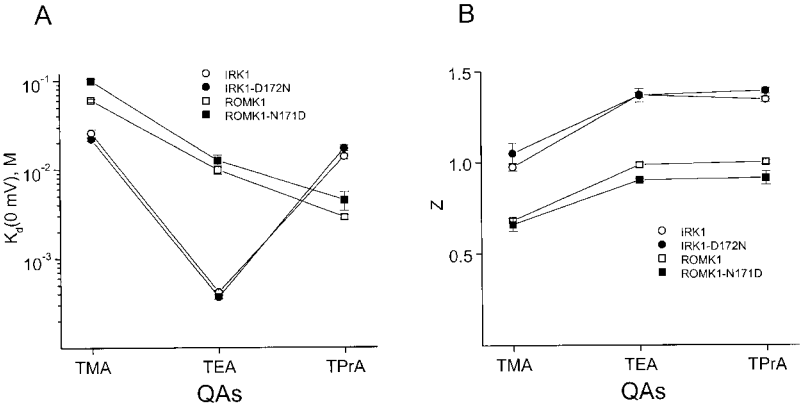

FIGURE 12. Comparison of equilibrium dissociation constants and associated valence factors for QA block of wild-type and mutant channels. The K_d(0 mV) and Z value (mean ± SEM, $n = 5$) for each of three QAs tested are presented in A and B, respectively. (circles) IRK1; (squares) ROMK1. (open symbols) Wild-type channels; (closed symbols) mutant channels.

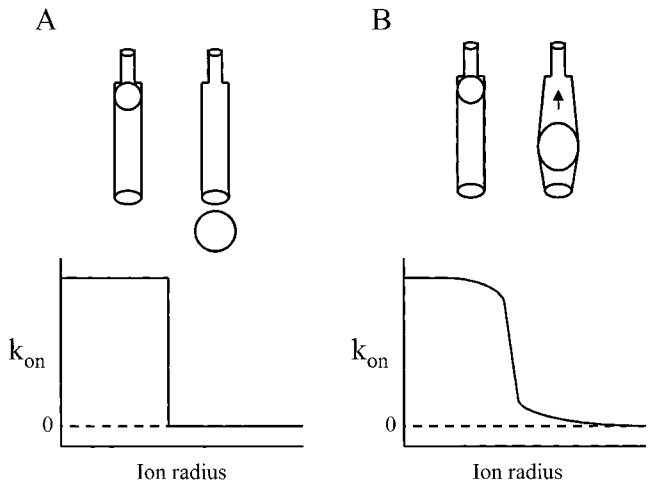

FIGURE 13. Models of QA entering the inner pore. The two systems are either without (A) or with (B) compliance and hindrance.

needs to determine not only whether ions of a given size can or cannot enter, but also the rates of entry. The compliance and hindrance of the system cause the ion entry rate to drop gradually with increasing ion radius, rather than abruptly as in the idealized system (Fig. 13). Furthermore, if compliance in the system is high relative to the radius range of available test ions, the experimental ion entry rate may not drop to zero, as occurred in the present study. Despite these complications, one can still infer the pore diameter from the expected steep drop of entry rate with increasing ion size.

As shown in Fig. 10, k_{on} decreases with increasing QA size, from 5×10^5 M^{-1} s^{-1} for TEA to 3×10^3 M^{-1} s^{-1} for TPeA. Limiting equivalent conductivities for TMA, TEA, TPrA, TBA, and TPeA are 45, 33, 23, 19, and 17 (S/cm)/(equiv/cm^3), respectively (Robinson and Stokes, 1968). Accepting some common assumptions, these values predict diffusion-limited k_{on} rates of 10^8–10^9 M^{-1} s^{-1} (Andersen, 1983a,b; Kuo and Hess, 1992a,b). Clearly, experimental k_{on} (0 mV) values for all QAs examined are well below those expected for a diffusion-limited process, which argues that the inner pore is spatially restricted. The "diameters" of TMA, TEA, TPrA, TBA, and TPeA are ~7, 8, 9, 10, and 11 Å, respectively (Robinson and Stokes, 1968). Therefore, as discussed above, the steep (30-fold) drop in k_{on} observed between TPrA and TBA, compared with two- to threefold drops between TEA and TPrA and between TBA and TPeA (Fig. 10 A), argues that the diameter of the inner pore is ~9 Å, which is comparable in the size to a K^+ ion with a single H_2O shell. Moreover, the value of k_{off} for QAs (except for TEA in IRK1) decreases with increasing alkyl chain length (Fig. 10 C), which is consistent with the notion that the path between the QA-binding locus and the intracellular solution is spatially restricted and that hydrophobic interaction is a crucial factor in channel–QA interaction. It should be noted (Fig. 10 A) that both the absolute value of k_{on} for a given QA and its variation with QA size are nearly the same in IRK1 and ROMK1, which argues that the inner pores of these two channels likely share some common architectural features, despite the fact that rectification is strong in the former and weaker in the latter.

We thank L.Y. Jan for IRK1 cDNA, K. Ho and S. Hebert for ROMK1 cDNA, P. De Weer for critical review and discussion of our manuscript, and C.M. Armstrong for helpful discussion.

This study was supported by the National Institutes of Health grant No. GM55560 (to Z. Lu). Z. Lu was a recipient of an Independent Scientist Award from NIH (No. HL03814).

Submitted: 8 December 2000
Revised: 26 March 2001
Accepted: 27 March 2001

REFERENCES

Andersen, O.S. 1983a. Ion movement through gramicidin A channels: single-channel measurements at very high potentials. *Biophys. J.* 41:119–133.

Andersen, O.S. 1983b. Ion movement through gramicidin A channels: studies on the diffusion-controlled association step. *Biophys. J.* 41:147–165.

Armstrong, C.M. 1971. Interaction of tetraethylammonium ion derivatives with the potassium channels of giant axons. *J. Gen. Physiol.* 58:413–437.

Armstrong, C.M., and L. Binstock. 1965. Anomalous rectification in the squid giant axon injected with tetraethylammonium chloride. *J. Gen. Physiol.* 48:859–872.

Choi, K.L., C. Mossman, J. Aube, and G. Yellen 1993. The internal quaternary ammonium receptor site of *Shaker* potassium channels. *Neuron.* 10:533–541.

del Camino, D., M. Holmgren, Y. Liu, and G. Yellen. 2000. Blocker protection in the pore of a voltage-gated K^+ channel and its structural implications. *Nature.* 403:321–325.

Doyle, D.A., C.J. Morais, R.A. Pfuetzner, A. Kuo, J.M. Gulbis, S.L. Cohen, B.T. Chait, and R. MacKinnon. 1998. The structure of the potassium channel: molecular basis of K^+ conduction and selectivity. *Science.* 280:69–77.

Fakler, B., U. Brandle, E. Glowatzki, S. Weidemann, H.P. Zenner, and J.P. Ruppersburg. 1995. Strong voltage-dependent inward-rectification of inward-rectifier K^+ channels is caused by intracellular spermine. *Cell.* 80:149–154.

Ficker, E., M. Taglialatela, B.A. Wible, C.M. Henley, and A.M. Brown. 1994. Spermine and spermidine as gating molecules for inward rectifier K^+ channels. *Science.* 266:1068–1072.

French, R.J., and J.J. Shoukimas. 1981. Blockage of squid axon potassium conductance by internal tetra-N-alkylammonium ions of various sizes. *Biophys. J.* 34:271–291.

Guo, D., and Z. Lu. 2000. Pore block versus intrinsic gating in the mechanism of inward rectification in strongly rectifying IRK1 channels. *J. Gen. Physiol.* 116:561–568.

Hille, B. 1971. The permeability of the sodium channel to organic cations in myelinated nerves. *J. Gen. Physiol.* 58:599–619.

Ho, K., C.G. Nichols, W.J. Lederer, J. Lytton, P.M. Vassilev, M.V. Kanazirska, and S.C. Hebert. 1993. Cloning and expression of an inwardly rectifying ATP-regulated potassium channel. *Nature.* 362:31–38.

Holmgren, M., P.L. Smith, and G. Yellen. 1997. Trapping of organic blockers by closing of voltage-dependent K^+ channels: evidence for a trap door mechanism of activation gating. *J. Gen. Physiol.*

109:527–535.

Kubo, Y., T.J. Baldwin, Y.N. Jan, and L.Y. Jan. 1993. Primary structure and functional expression of a mouse inward rectifier potassium channel. *Nature.* 362:127–133.

Kuo, C.-C., and P. Hess. 1992a. A functional view of the entrances of L-type Ca^{2+} channels: estimates of the size and surface potential at the pore mouths. *Neuron.* 9:515–526.

Kuo, C.-C., and P. Hess. 1992b. Ion permeation through the L-type Ca^{2+} channel in rat phaeochromocytoma cells: two sets of ion binding sites in the pore. *J. Physiol.* 466:629–655.

Lopatin, A.N., E.N. Makhina, and C.G. Nichols. 1994. Potassium channel block by cytoplasmic polyamines as the mechanism of intrinsic rectification. *Nature.* 372:366–369.

Loussouarn, G., E.N. Makhina, T. Rose, and C.G. Nichols. 2000. Structure and dynamics of the pore of inwardly rectifying K_{ATP} channels. *J. Biol. Chem.* 275:1137–1144.

Lu, T., B. Nguyen, X. Zhang, and J. Yang. 1999. Architecture of a K^+ channel inner pore revealed by stoichiometric covalent modification. *Neuron.* 22:571–580.

Lu, Z., and R. MacKinnon. 1994. Electrostatic tuning of Mg^{2+} affinity in an inward-rectifier K^+ channel. *Nature.* 371:243–246.

Oliver, D., H. Hahn, C. Antz, J.P. Ruppersberg, and B. Fakler. 1998. Interaction of permeant and blocking ions in cloned inward-rectifier K^+ channels. *Biophys. J.* 74:2318–2326.

Robinson, R.A., and R.H. Stokes. 1968. Electrolyte Solutions. 2nd edition. The Butterworths Group, London. 577 pp.

Spassova, M., and Z. Lu. 1998. Coupled ion movement underlies rectification in an inward-rectifier K^+ channel. *J. Gen. Physiol.* 112:211–221.

Spassova, M., and Z. Lu. 1999. Tuning the voltage dependence of tetraethylammonium block with permeant ions in an inward-rectifier K^+ channel. *J. Gen. Physiol.* 114:415–426.

Stanfield, P.R., N.W. Davies, P.A. Shelton, M.J. Sutcliffe, I.A. Khan, W.J. Brammer, and E.C.J. Conley. 1994. A single aspartate residue in involved in both intrinsic gating and blockage by Mg^{2+} of the inward-rectifier, IRK1. *J. Physiol.* 478:1–6.

Woodhull, A.M. 1973. Ionic blockage of sodium channels in nerve. *J. Gen. Physiol.* 61:687–708.

Yang, J., Y.N. Jan, and L.Y. Jan. 1995. Control of rectification and permeation by residues in two distinct domains in an inward rectifier K^+ channel. *Neuron.* 14:1047–1054.